frontiers | Frontiers in Earth Science

TYPE Original Research
PUBLISHED 13 September 2022
DOI 10.3389/feart.2022.866304

Check for updates

OPEN ACCESS

EDITED BY
Zhang Chengjun,
Lanzhou University, China

REVIEWED BY
Hui Tian,
State Key Laboratory of Organic Geochemistry, Guangzhou Institute of Geochemistry (CAS), China
Junsheng Nie,
Lanzhou University, China

*CORRESPONDENCE
Zhifu Wei,
weizf@lzb.ac.cn

SPECIALTY SECTION
This article was submitted to Quaternary Science, Geomorphology and Paleoenvironment, a section of the journal Frontiers in Earth Science

RECEIVED 31 January 2022
ACCEPTED 15 August 2022
PUBLISHED 13 September 2022

CITATION
Li S, Ma X, Jiang S, Wang G, Zhang T, He W, Yu X, Ma H, Zhang P, Wei J, Wang Y and Wei Z (2022), Long-term drying trend during 51.8–37.5 Ma in the Nangqian Basin, central-eastern Qinghai–Tibet Plateau.
Front. Earth Sci. 10:866304.
doi: 10.3389/feart.2022.866304

COPYRIGHT
© 2022 Li, Ma, Jiang, Wang, Zhang, He, Yu, Ma, Zhang, Wei, Wang and Wei. This is an open-access article distributed under the terms of the Creative Commons Attribution License (CC BY). The use, distribution or reproduction in other forums is permitted, provided the original author(s) and the copyright owner(s) are credited and that the original publication in this journal is cited, in accordance with accepted academic practice. No use, distribution or reproduction is permitted which does not comply with these terms.

Long-term drying trend during 51.8–37.5 Ma in the Nangqian Basin, central-eastern Qinghai–Tibet Plateau

Shangkun Li[1,2], Xueyun Ma[1], Shaohua Jiang[3], Gen Wang[1], Ting Zhang[1], Wei He[1], Xiaoli Yu[1,2], He Ma[2,4], Pengyuan Zhang[2,4], Jingyi Wei[2,4], Yongli Wang[4] and Zhifu Wei[1]*

[1]Key Laboratory of Petroleum Resources Research, Northwest Institute of Eco-Environment and Resources, Chinese Academy of Sciences, Lanzhou, China, [2]University of Chinese Academy of Sciences, Beijing, China, [3]Weifang Vocational College, Weifang, China, [4]Key Laboratory of Cenozoic Geology and Environment, Institute of Geology and Geophysics, Chinese Academy of Sciences, CAS Center for Excellence in Life and Paleoenvironment, Beijing, China

Since the Cenozoic, the earth entered a period of relatively active tectonic movement, which led to significant environmental and climatic shifts, including inland drought in Asia, global cooling, and the formation of the Asian monsoon. The Asian aridification has a far-reaching impact on the human living environment, and so do the climate changes in China. The beginning, strengthening, and ending times of the inland drought in Asia have been a long-concerned issue. Therefore, it is necessary to reveal the starting time, evolution process, and underlying driving mechanisms. Because of its unique topography and geographical location, the Qinghai–Tibet Plateau is known as the "starter" and "amplifier" of global climate change. It is a key area and an ideal "laboratory" for long-time scale climate change. Located in the central-eastern part of the Qinghai–Tibet Plateau, the Nangqian Basin is not only the confluence area of major monsoons and westerly winds but also the boundary between humid and arid areas. Moreover, the Nangqian section in the basin has a long continuous sedimentary sequence, making it a good carrier for long-time scale climate change research. In this study, biomarkers and total organic carbon (TOC) in the sedimentary strata of the Nangqian Basin in the central-eastern Qinghai–Tibet Plateau were used to reconstruct the paleoclimate and paleovegetation evolution history over the time interval of 51.8–37.5 Ma. According to the climatic index of the Nangqian Basin, the climate evolution history can be divided into three stages. StageI: during 51.8–46.4 Ma, the depositional environments at this stage were mainly a braided river and an ephemeral shallow pond/lake environment. Also, the value of CPI, $\delta^{13}C_{n\text{-alkanes}}$, and total organic carbon (TOC) was low; meanwhile, ACL value increased with nC_{27}/nC_{31} decrease, and these obvious change trends might be affected by the mixing of terrestrial sediments brought by rivers. The main peak carbons were nC_{22} and nC_{23}, the vegetation type was predominantly woody plants, and the climate was relatively humid. Stage II: during 46.4–42.7 Ma, Paq and nC_{27}/nC_{31} values decreased gradually, and ACL, $\delta^{13}C_{n\text{-alkanes}}$, and CPI values increased slowly. Also, the main peak carbon number changed from low to high, and the vegetation type varied from

woody to herbaceous. All these proxies displayed that the climate became more arid. Stage III: during 42.7–37.5 Ma, Paq, ACL, and nC_{27}/nC_{31} values did not vary too much, $\delta^{13}C_{n\text{-alkanes}}$ values increased slightly, and ACL values decreased slightly, while the main peak carbon number, TOC, and CPI increased significantly, indicating that the climatic conditions continued to get dryer, which may have been affected by the MECO events. In addition, through the comparative study of the climate evolution history of the Eocene in the Nangqian Basin reconstructed by the multi-index system, together with the climate change in the adjacent area, the retreat process of the Paratethys Sea, the global deep-sea oxygen isotopes, and the global atmospheric CO_2 concentration, it is considered that the Eocene climate change in the Nangqian Basin is mainly affected by the global climate change and the retreat of the Paratethys Sea. The uplift of the Qinghai–Tibet Plateau and the increase of altitude have little influence on the water vapor of the Nangqian Basin, and the basin was rarely affected by the South Asian monsoon.

KEYWORDS

biomarkers, paleoclimate, paleovegetation, Nangqian Basin, Qinghai–Tibet Plateau

1 Introduction

With the collision between the Eurasian plate and the Indian plate during the Paleocene–Eocene, the Qinghai–Tibet Plateau uplifted into the largest plateau with the highest elevation in the world (Fielding et al., 1994). At present, the Qinghai–Tibet Plateau is about 2,800 km long from east to west and 300–1,500 km wide from north to south. Also, it covers a total area of 2.5 million square kilometers, nearly accounting for about 25% of China's total area. The Qinghai–Tibet Plateau with an average elevation above 4,000 m covers an area of 1.22 million square kilometers, making it known as the "third pole of the world." The Qinghai–Tibet Plateau receives intense solar radiation due to its large area, low relative latitude, and high altitude. Due to these special reasons, the Qinghai–Tibet Plateau can absorb water from the Indian Ocean to the north in summer, while the mid-latitude atmospheric jet stream from the northwest exerts a strong influence on the plateau environment in winter. In addition, due to the high altitude and cold climate conditions (annual average temperature <4°C), the ecological environment of the Qinghai–Tibet Plateau is fragile and the response to climate change is more intense than that of most regions on Earth (Liu et al., 2009).

Because of its unique topography and geographical position, the Qinghai–Tibet Plateau is known as the "starting motor" and "amplifier" of global climate change. It is a key area of global change research and an ideal "laboratory" for long-term climate change research and has become the focus of attention of geoscientists all over the world. The climate change on the Qinghai–Tibet Plateau during the Cenozoic has triggered many discussions and is an important part of climate change in Central Asia. The study of climate change on the Qinghai–Tibet Plateau is an indispensable process for understanding the generation and development of Asian aridity and monsoon and is also of great significance to the understanding of marine chemistry and global climate change (Raymo et al., 1988; Ruddiman and Kutzbach, 1991; Edmond, 1992; An et al., 2001; Molnar, 2005; Harris, 2006).

Due to the lack of long and continuous deposition, previous studies on the climate evolution of the Qinghai–Tibet Plateau over the Cenozoic were mostly focused on the late Cenozoic. In addition, studies on the climate evolution of the Qinghai–Tibet Plateau are mostly concentrated on the northeast, central, and southern parts of the Qinghai–Tibet Plateau (Sorrel et al., 2017; Yuan et al., 2016; Miao et al., 2016; Su et al., 2018; Wei et al., 2017), while there are few studies on the long-term climate change in the Nangqian Basin in the central-eastern part of the Qinghai–Tibet Plateau. Moreover, the methods like palynology and clay minerals were mainly used in the analysis (Yuan et al., 2016; Zhao et al., 2020), supplemented grain size analysis, and sedimentary changes (Yuan et al., 2020; Fang et al., 2021). However, the original biological information recorded by biomarker compounds can be verified by multiple indicators from various angles, so as to more accurately reflect the evolutionary history of palaeovegetation and palaeoclimate in the study area. The Nangqian Basin profile selected for this study has a long continuous sedimentary sequence and is an ideal sedimentary profile for studying the climatic evolution of the whole Eocene. In addition, Zhang et al. (2020) used magnetic stratigraphy and determined the age model of the Nangqian Basin profile, which laid an important foundation for the reconstruction of the Nangqian Basin climatic conditions and vegetation evolution (Zhang et al., 2020).

Biomarker compounds are derived from organisms and retain the basic carbon skeleton of organic compounds inherent in organisms, with advantages such as good stability,

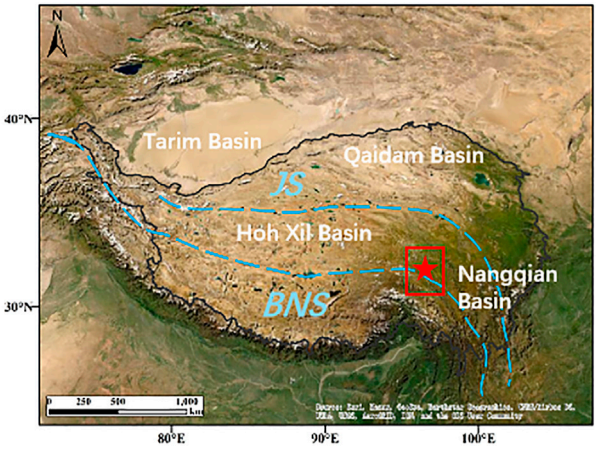

FIGURE 1
Geographical location map of the Nangqian Basin.

long preservation time, and wide application range (Xie et al., 2003a). *n*-alkanes extracted from plant leaf waxes can be preserved in sediments for a long time, and thus, can record palaeovegetation change information (Zhang et al., 2006). At present, the use of biomarkers has become an important method to reconstruct paleoclimate and paleoenvironment. The reconstruction of the paleoclimate environment by biomarker compounds has been widely applied in marine sediments, lakes, peat sediments, and loess-paleosol (Cranwell et al., 1987; Xie et al., 2003b). The reconstruction of paleoclimate and vegetation evolution using biomarkers in the Nangqian Basin in the central and eastern part of the Qinghai–Tibet Plateau is still absent. In this study, biomarkers, TOC, and carbon isotope $\delta^{13}C$ of *n*-alkanes from the sediments of the Nangqian Basin in the central-northeastern Qinghai–Tibet Plateau were used to reconstruct the paleoclimate and paleovegetation evolution history during 51.8–37.5 Ma. Our study provides important geological evidence for clarifying the Paleocene climate evolution in the central-east Qinghai–Tibet Plateau.

2 Study area

The Nangqian Basin is located at the junction of Qinghai Province and the Tibet Autonomous Region, northeast of the central area of the Qinghai–Tibet Plateau, it is the tectonic transition and bending part of the Qinghai–Tibet Plateau; the regional tectonic activity changes from east-west to north-south as well. The basin, with an average elevation of about 4,500–5,000 m, was formed by the Paleogene compression process after the Indo-Asian plate collision (Horton et al., 2002). The Nangqian Basin belongs to the Qiangtang Block, which is bound by the Jinsha Suture and Songpan-Ganzi Block in the north and Bangong-Nujiang Suture and Lhasa Block in the south, at 32°00′ N - 32°20′ N and 96°15′ E - 96°45′ E, respectively (Figure 1). The study area has a continental monsoon climate, with long cold winters and short rainy summers. The climate is cool and the annual precipitation mainly concentrates from June to September. At the same time, the basin and its adjacent areas are also a key part of the reorganization of large river systems, the evolution of monsoons, and biodiversity (Su et al., 2018).

The sedimentary facies gradually developed from braided river and alluvial fan to ephemeral pool/lake environment and finally evolved into brackish lake deposits. At the same time, this succession also reflects that the deposition in the early stage of the Nangqian Basin was influenced by the Jinsha Suture caused by the collision and compression of the Indo-Asian Plate, and the overall climatic conditions gradually became arid. The sedimentary environment of such saline lakes was generally well developed in the semi-arid area of northwest China during the Upper Quaternary (Fang et al., 2021).

3 Materials and methods

3.1 Sampling and profile chronology

In this study, the profile chronology data came from the paleomagnetic chronology measured by Zhang Weilin in the Institute of Qinghai–Tibet Plateau Research, Chinese Academy of Sciences (Zhang et al., 2020). The Nangqian profile is divided into NQ2, NQ, and NQ1 sections for sampling from bottom to top. There are 28 samples in the NQ2 section, 13 samples in the NQ1 section, 26 samples in the NQ section, and 67 samples in total.

In the NQ section, some samples are missing because of the unoutcroped stratum of about 150–200 m, the latest sample in this study is NQ1-242. The length of the section stratigraphic map is based on Zhang's section length (Zhang et al., 2020). There is a wide range of red bed sequences in the sampled strata, and the lithologic variation trend is roughly represented as follows: paleosoil sandstone in the lower part, limestone–marl in the middle part, and siltstone–mudstone in the upper part with obvious gypsum layers, which also reflects a climate condition gradually changing from semi-arid to arid (Figure 2); the age range is approximately 51.8–37.5 Ma BP.

3.2 Determination of total organic carbon content

The sample was ground to more than 80 mesh using an agate mortar before testing for organic carbon content. 0.20 g powder samples were weighed using an electronic balance with an accuracy of 1/10,000 and placed in a quartz crucible. Before the sample was tested on the machine, the measured samples

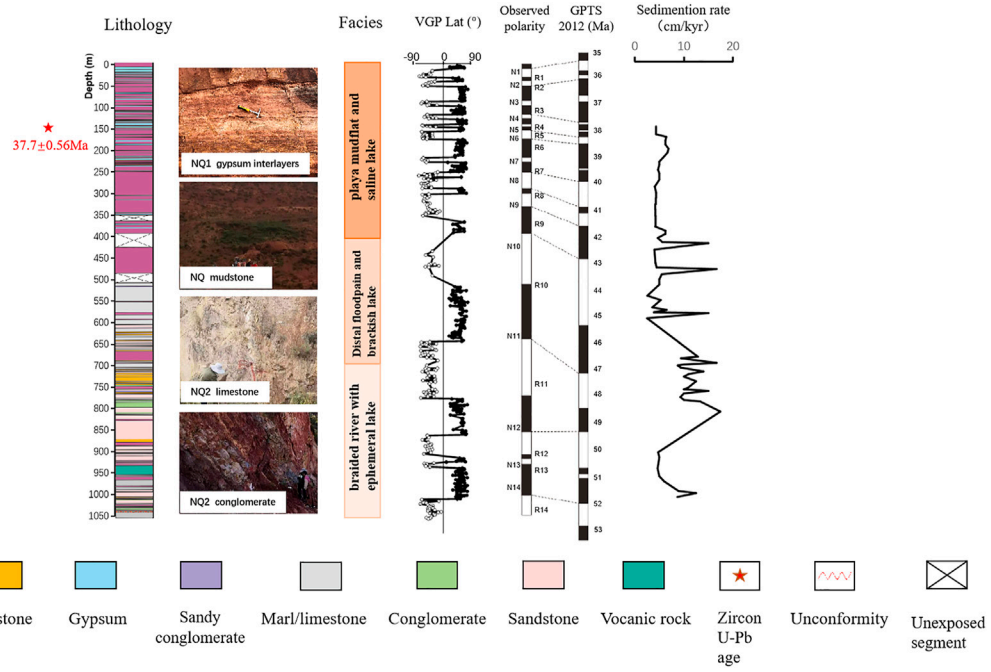

FIGURE 2
Sampling and chronological map of the Nangqian Basin.

were soaked with 6% hydrochloric acid for 24 h and acidified to remove inorganic carbon. After rinsing with deionized water to neutralize it and then drying it in an oven at 40°C, the crucible containing the sample was placed on the combustion table of the instrument, and the CO_2 production was measured by using an infrared detector to calculate the total organic carbon (TOC) content of each sample. The samples were pretreated and tested in the Key Laboratory of Petroleum Resources Research of Gansu Province, Northwest Institute of Eco-Environment and Resources, Chinese Academy of Sciences. The instrument was LECOCS900 carbon and sulfur analyzer.

3.3 *n*-Alkanes and compound-specific carbon isotope analysis

A total of 67 samples were collected in this study with an interval of about 10 m. Organic matter was extracted by a traditional Soxhlet extraction device, and the extracted organic matter was used for organic geochemical analysis. Before extraction, the sample was ground to 100–200 meshes, the extraction solvent was methylene chloride and methanol (v: v=9:1), and the extraction time was 72 h. The extracted organic matter and solvent mixture samples were evaporated and concentrated by nitrogen purging, then, n-hexane was further used as an extraction solvent, and the saturated hydrocarbon components were extracted several times using silica gel and alumina as fillers. The saturated hydrocarbon components were dried and diluted with $CHCl_3$ and analyzed by gas chromatography-mass spectrometry (GC-MS), and the n-alkane spectra of mass-nucleus ratio m/z=57 and m/z=85 were obtained. Then, the relative content of *n*-alkanes in the sample was obtained. The same procedure is used to check blank samples during testing to monitor for contamination.

Test instrument conditions: gas chromatography-mass spectrometer model HP6890GC/5973MS; the capillary column was an HP-5MS quartz capillary column (30mm×0.25mm×0.25 μm). The carrier gas was high-purity helium. The carrier gas flow rate was 1.2 ml/min, and the carrier gas linear velocity was 40 cm/s. The initial temperature of the column is 80°C, the temperature rises by 3°C per minute, the final temperature is 300°C, and the final temperature is kept constant for 20 min. The ion source was EI, the ionization energy was 70 eV, the ion source temperature was 280°C, and the interface between mass spectrometry and chromatography was 280°C.

The compound-specific carbon isotope was determined using a gas chromatography-isotope ratio mass spectrometry (Thermo Scientific MAT253). The experiments were completed in Gansu Key Laboratory of Oil and Gas Resources Research, Northwest Institute of Eco-Environment and Resources, Chinese Academy of Sciences.

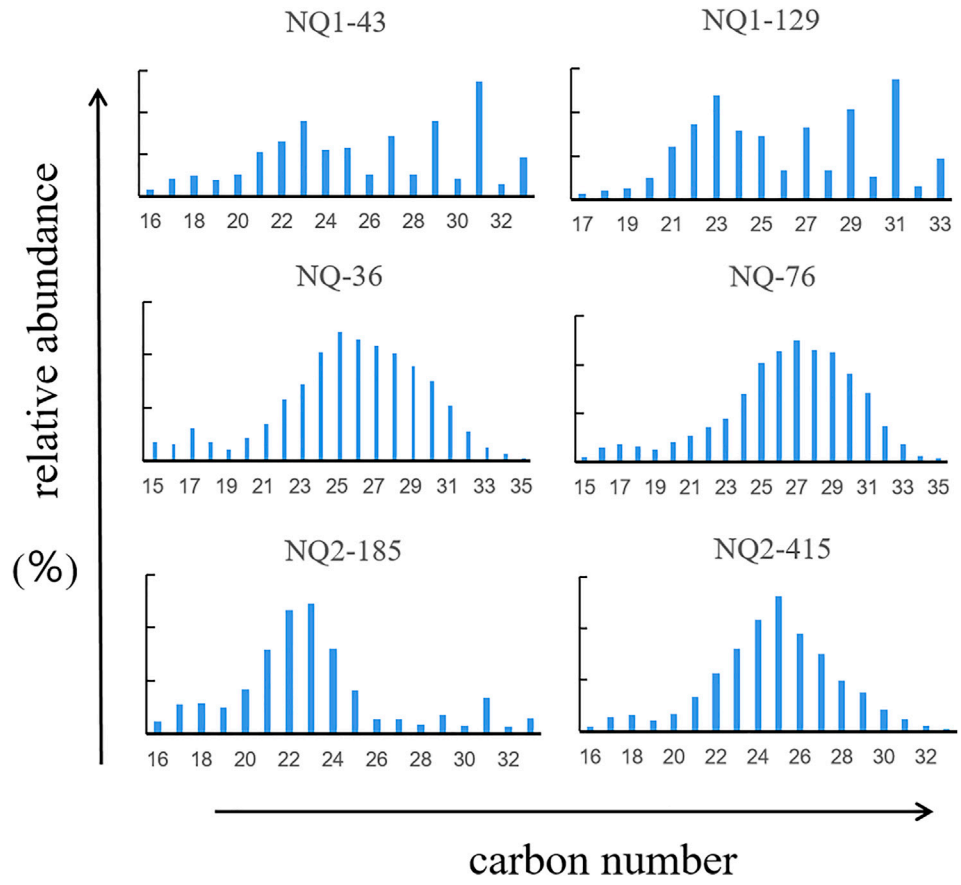

FIGURE 3
Distribution map of *n*-alkanes in Nangqian samples.

4 Results

4.1 Analysis of biomarker compounds

The distribution characteristics of *n*-alkanes in 67 samples from the Nangqian section are shown in Figure 3. The carbon number of *n*-alkanes is distributed between nC_{15} and nC_{33}. For the NQ2 section, their peak patterns can be roughly divided into two types. Among them, 21 samples from NQ2-15 to NQ2-360 show a bimodal distribution pattern, with nC_{22} and nC_{23} as the main peak carbon. A total of seven samples from NQ2-370 to NQ2-483 were distributed in a single-peak pattern, and the main peak carbon was nC_{25}. For the NQ section, the peak patterns were a single-peak distribution, and the main peak carbons are nC_{25} and nC_{26}. For the NQ1 section, which was distributed in a bimodal pattern, nC_{23} was the main peak carbon in the front peak part and nC_{31} was the main peak carbon in the back peak part. The high carbon number part had an obvious odd carbon advantage.

In this study, nC_{27}/nC_{31}, average carbon chain length (ACL) of *n*-alkanes ($C > nC_{25}$), carbon dominance index (CPI) of *n*-alkanes ($C > nC_{23}$), and relative input index of *n*-alkanes of aquatic plants Paq were selected, as well as Pr/Ph, $\sum$ n-C_{21} -/$\sum$ n-C_{22} +, etc., the corresponding calculation formula is as follows:

$$ACL_{27\text{-}31}=(27\times nC_{27}+29\times nC_{29}+31\times nC_{31}+33\times nC_{33})/(nC_{27}+nC_{29}+nC_{31}+nC_{33})$$ (Fang et al., 2021)

$$CPI=0.5\times[(nC_{23}+nC_{25}+nC_{27}+nC_{29}+nC_{31})/(nC_{22}+nC_{24}+nC_{26}+nC_{28}+nC_{30})+(nC_{23}+nC_{25}+nC_{27}+nC_{29}+nC_{31})/(nC_{24}+nC_{26}+nC_{28}+nC_{30}+nC_{32})]$$ (Ficken et al., 2000)

$$Paq=(nC_{23}+nC_{25})/(nC_{23}+nC_{25}+nC_{29}+nC_{31})$$ (Eglinton and Hamilton, 1967)

As shown in Figure 4 and Table 1, CPI values of Nangqian profile samples ranged from 1.02 to 3.54, with an average of 1.65. $\sum$ n-C_{21} -/$\sum$ n-C_{22} + values range from 0.06 to 0.73, with an average of 0.27; Paq values ranged from 0.26 to 0.93, with an average of 0.61. ACL values ranged from 27.11 to 30.25, with an

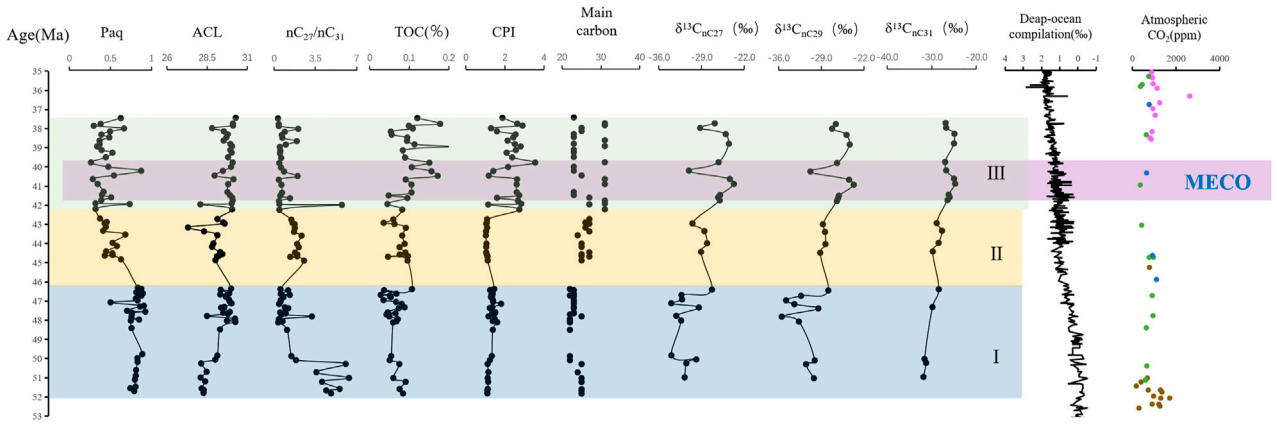

FIGURE 4
Comparison of *n*-alkane-derived indices in the Nangqian section.

average of 29.05. nC_{27}/nC_{31} ranged from 0.33 to 6.35, with an average of 1.55. nC_{17}/nC_{31} values ranged from 0.01 to 4.57, with an average value of 0.59.

4.2 Analysis of total organic carbon content

In this study, TOC data of 60 samples were obtained by measuring and removing outliers (Table 1), with a content range of 0.03–0.20% and an average value of 0.08%.

4.3 Carbon isotope analysis of *n*-alkanes

In this study, 28 *n*-alkanes samples from 51.8 to 37.5 Ma, were selected for carbon isotope analysis of *n*-alkanes. As shown in Figure 4 and Table 2, the carbon isotopes of *n*-alkanes nC_{23} and nC_{25} in the Nangqian Basin range from 39.0‰ to 29.5‰ and from 35.1‰ to 26.1‰, respectively. In long chain alkanes variation range of carbon isotopes were 34.0–23.7‰ (nC_{27}), 35.5–23.7‰ (nC_{29}), 31.9–24.8‰ (nC_{31}), and 31.6–24.5‰ (nC_{33}) (table 2). On the whole, the long-chain and middle-chain *n*-alkanes isotopes in the Nangqian Basin show a trend of gradual increase on a long-term temporal scale and a certain degree of periodic fluctuation in a short period. The carbon number range of carbon isotope results of *n*-alkanes obtained in this study includes nC_{17}-nC_{33}, but the experimental results of low carbon number part and high carbon number part were missing, and the GC-MS results of *n*-alkanes also indicate that the trend of long-chain *n*-alkanes (ACL) is relatively obvious, so we use the data to get more complete results. Long-chain *n*-alkanes nC_{27}–nC_{31}, represent the range of carbon numbers in higher plants as an indicator of climate change.

In 2010, Aichner analyzed the distribution and carbon isotopes of *n*-alkanes in aquatic plants and lake surface sediments from 40 lakes in the central and eastern Qinghai–Tibet Plateau (Aichner et al., 2010) and concluded that ^{13}C produced by mid-chain alkanes from aquatic plants are richer than long-chain alkanes produced by land plants. This is because some aquatic plants in the lake can use HCO^{3-} for metabolism, and HCO^{3-} is more enriched in ^{13}C than in dissolved CO_2.

However, in the sediments of fluvial and lacustrine facies profiles in the Nangqian Basin, the middle-chain *n*-alkanes (nC_{23} and nC_{25}) of most samples are more depleted than long-chain *n*-alkanes (nC_{27}-nC_{33}) in ^{13}C (Figure 4). This phenomenon has also been found in the surface sediments of Lake Challa in tropical Africa. The carbon isotopes of medium alkanes (nC_{23} and nC_{25}) in the surface sediments of Lake Challa range from -30‰ to -48‰. Lake Challa is a crater lake with a steep slope at the bottom and no shallow water suitable for the growth of aquatic plants. Therefore, the authors believe that medium alkanes may not come from aquatic plants. However, the specific source of alkanes is not given (Damsté et al., 2011). In Xiaolongwan Lake in northeast China, the δ13C values of middle-chain *n*-alkanes in lake sediments are more negative than those of long-chain *n*-alkanes. This phenomenon is explained by the authors as follows: under the environmental conditions of anoxia at the lake bottom, methanogens decompose organic matter to produce methane and CO_2. With the seasonal flow of lake water, CO_2 enters the shallow water layer and is utilized by aquatic plants, resulting in the relatively depleted ^{13}C in middle-chain *n*-alkanes (Sun et al., 2013).

TABLE 1 Organic geochemical index parameters of samples from the Nangqian Basin.

Sample ID	CPI	$\Sigma nC_{22}^-/\Sigma nC_{22}^+$	Paq	Pr/Ph	G/$C_{30}H$	nC_{17}/nC_{31}	nC_{27}/nC_{31}	ACL	TOC (%)	Carbon peak
NQl-242	1.87	0.38	0.63	0.31	0.15	0.34	0.33	29.14	0.12	23
NQl-229	2.63	0.31	0.38	0.37	0.13	0.21	0.40	29.50	0.18	31
NQl-222	2.89	0.15	0.30	0.20	0.07	0.04	0.40	29.59	0.10	31
NQl-213	1.29	0.10	0.67	0.39	0.06	0.21	2.04	27.31	0.11	25
NQl-203	1.59	0.06	0.50	0.10	0.12	0.01	0.90	28.30	0.05	25
NQl-192	2.54	0.15	0.39	0.17	0.14	0.04	0.65	29.13	0.06	23
NQl-182	2.43	0.19	0.49	0.39	0.11	0.13	0.70	28.89	0.09	23
NQl-172	2.13	0.34	0.37	0.45	0.13	0.34	1.92	28.80	0.09	31
NQl-163	2.51	0.42	0.37	0.41	0.11	0.38	0.99	29.30	0.11	23
NQl-157	2.80	0.16	0.34	0.28	0.09	0.07	0.49	29.45	0.20	31
NQl-148	2.56	0.13	0.39	0.26	0.17	0.04	0.53	29.24	0.08	23
NQl-141	2.09	0.33	0.52	0.34	0.13	0.29	0.50	29.11	-	23
NQl-129	2.37	0.15	0.44	0.20	0.09	0.05	0.60	29.01	0.09	23
NQl-118	3.54	0.17	0.26	0.31	0.05	0.07	0.44	29.62	0.15	31
NQl-108	2.16	0.29	0.47	0.30	0.09	0.23	0.58	29.25	0.11	23
NQl-99	1.40	0.70	0.87	0.45	0.14	4.05	0.85	27.12	0.16	23
NQl-89	1.17	0.09	0.54	0.24	0.20	0.16	1.99	27.85	0.17	25
NQl-81	2.62	0.14	0.29	0.27	0.37	0.06	0.40	29.67	0.09	31
NQl-70	2.60	0.15	0.34	0.28	0.11	0.05	0.62	29.18	0.11	31
NQl-53	2.60	0.29	0.42	0.39	0.12	0.26	0.67	29.00	0.11	23
NQl-43	2.73	0.26	0.40	0.31	0.10	0.15	0.52	29.21	0.05	23
NQl-35	1.59	0.53	0.51	0.36	0.20	0.75	1.35	28.09	0.10	27
NQl-28	2.66	0.42	0.39	0.41	0.04	0.34	0.41	29.44	-	31
NQl-19	2.83	0.31	0.32	0.32	0.13	0.19	0.45	29.46	0.04	19

"-" means lower than the detection limit or abnormal value, no data.

5 Discussion

5.1 Source of organic matter

The organic matter in lake sediments can be divided into two sources: one is from imported land higher plants and another is the endogenous aquatic organisms from the water body, which are mainly composed of lower bacteria, algae, and aquatic plants (emergent, submerged, and floating plants) (Dodd and Afzal-Rafii, 2000). The distribution range of *n*-alkanes carbon number in terrestrial higher plants is generally between nC_{15} and nC_{33}, with nC_{27}, $nC_{29,}$ or nC_{33} as the main peak, which has an obvious odd-carbon advantage. The distribution range of *n*-alkanes carbon number in lower bacteria and algae is generally between nC_{15} and nC_{17}, with nC_{17} as the main peak and single-peak type distribution, without obvious odd-carbon advantage (Eglinton and Hamilton, 1967). The carbon number distribution of submerged/floating plants is generally between nC_{21} and nC_{25}, while the distribution of *n*-alkanes in emergent plants and higher plants is similar, and the bimodal distribution is considered to be the mixed source (Dodd and Afzal-Rafii, 2000).

Previous studies have proposed that the sediment Paq value can indicate the proportion of *n*-alkanes input by submerged/floating plants in *n*-alkanes with high carbon numbers. It is generally believed that when the Paq value is less than 0.1, terrigenous higher plants are the main biological sources; when the Paq value is between 0.1 and 0.4, emergent plants are the main biological sources; when Paq value is between 0.4 and 1.0, the main biological source is submerged/floating aquatic macrophytes (Ficken et al., 2000).

In addition, for the two indices of $\sum$ n-$C_{21}^-/\sum$ n-C_{22}+ and nC_{17}/nC_{31}, it is believed that they can also indicate the proportion of lower aquatic bacteria and algae to higher plants. $nC_{17}/nC_{31}<0.5$ indicates that higher plants are the main inputs, and $nC_{17}/nC_{31}>2$ indicates that bacteria and algae are the main inputs (Xie et al., 2005; Xie et al., 1999).

Therefore, according to the abovementioned indicators, we can divide the whole period into three stages to discuss the source of organic matter. In the first stage, 51.8–46.4 Ma, Paq is 0.8,

TABLE 2 Compound-specific carbon isotope of samples from the Nangqian Basin.

Sample ID	Age (Ma)	$\delta13C_{nC23}$	$\delta13C_{nC25}$	$\delta13C_{nC27}$	$\delta13C_{nC29}$	$\delta13C_{nC31}$
NQ-87	35.59	-36.7	-32.3	-30.5	-28.7	-28.9
NQ-66	35.96	-31.7	-29.5	-28.5	-28.4	-27.7
NQ-45	36.5	-31.2	-29.2	-28.1	-28.3	-28.5
NQ-26	36.99	-32.3	-30.4	-29.1	-29.2	-29.8
NQ-1-229	38.09	-33.0	-30.4	-26.8	-26.6	-26.9
NQ-1-213	38.31	-31.6	-30.9	-29.2	-27.2	-26.8
NQ-1-192	38.66	-29.9	-26.9	-25.0	-24.8	-24.9
NQ-1-163	39.23	-30.2	-26.3	-24.5	-24.3	-25.0
NQ-1-118	40.24	-29.8	-27.0	-26.2	-26.4	-27.0
NQ-1-99	40.69	-31.7	-31.1	-31.1	-30.8	-26.8
NQ-1-81	41.14	-31.9	-28.2	-24.4	-24.4	-25.0
NQ-1-70	41.38	-29.5	-26.1	-23.7	-23.7	-24.8
NQ-1-43	41.83	-30.1	-27.4	-26.0	-26.1	-26.2
NQ-1-35	42.01	-30.1	-27.3	-26.3	-26.2	-26.0
NQ-1-28	42.13	-30.9	-28.0	-26.0	-26.4	-26.5
NQ-2-415	47.34	-32.0	-32.3	-31.8	-30.2	-31.9
NQ-2-380	47.65	-31.8	-31.6	-31.5	-31.5	-31.3
NQ-2-370	47.75	-32.3	-30.0	-29.9	-30.1	-31.6
NQ-2-360	46.45	-33.7	-33.6	-33.9	-	-
NQ-2-272	48.64	-33.2	-35.1	-	-	-
NQ-2-196	49.37	-39.0	-34.7	-32.4	-32.7	-
NQ2-172	49.9	-34.4	-34.5	-33.1	-35.5	-
NQ-2-123	50.97	-30.6	-30.4	-29.4	-29.5	-29.8
NQ-2-100	51.23	-38.4	-31.0	-34.0	-33.4	-
NQ-2-75	51.54	-38.5	-34.1	-32.2	-34.8	-
NQ-2-54	51.77	-35.6	-34.9	-32.3	-32.3	-
NQ-2-24	52.15	-31.6	-30.4	-27.3	-27.8	-28.4

"-" means lower than the detection limit or abnormal value, no data.

nC_{17}/nC_{31} is 0.97, $\sum n\text{-}C_{21}^{-}/\sum n\ C_{22}+$ is 0.32, and the source of organic matter is mainly submerged/floating aquatic macroplants, with a small number of bacteria and algae input. The main carbon numbers were nC_{22} and nC_{23}. The distribution spectra of *n*-alkanes also show an obvious predominance of the front peak. Meanwhile, during 48.1–46.4 Ma, some *n*-alkanes with low content and high carbon number appeared back peak characteristics, which may be caused by the strong hydrodynamic conditions and the addition of small amounts of terrigenous organic matter.

The second stage is 46.4–42.7 Ma, in which the Paq value is 0.55, nC_{17}/nC_{31} is 0.34, and the $\sum n\text{-}C_{21}^{-}/\sum n\ C_{22}+$ is 0.18, indicating that the biological sources mainly changed from submerged/floating aquatic macrophytes to terrestrial higher plants, and the input of aquatic bacteria and algae is small. In the early period of this stage, the main carbon number is nC_{25} and it gradually transients to nC_{27} in the later period of this stage. The distribution spectra of *n*-alkanes also show an obvious unimodal pattern at this stage.

In the third stage, 42.7–37.5 Ma, Paq was relatively low, with an average of 0.44, and nC_{17}/nC_{31} had an average value of 0.38, indicating that the biological sources were mainly mixed inputs of submerged/floating aquatic macroplants and terrestrial higher plants. The average value of $\sum N\text{-}C_{21}\ -/\sum N\text{-}C_{22}\ +$ was 0.26, indicating that there was less input of aquatic bacteria and algae. The distribution spectrum of *n*-alkanes also showed a bimodal pattern at this stage, indicating that the source of organic matter was the aquatic-terrestrial mixed source.

5.2 Evolution of palaeovegetation

Modern molecular organic geochemical studies show that nC_{27} or nC_{29} is the main peak carbon in the distribution of *n*-alkanes when woody plants are dominant, and nC_{31} is the main peak carbon when herbaceous plants are dominant. The change in the nC_{27}/nC_{31} ratio can reflect the change in the relative content of woody and herbaceous plants. The increase in $nC_{27}/$

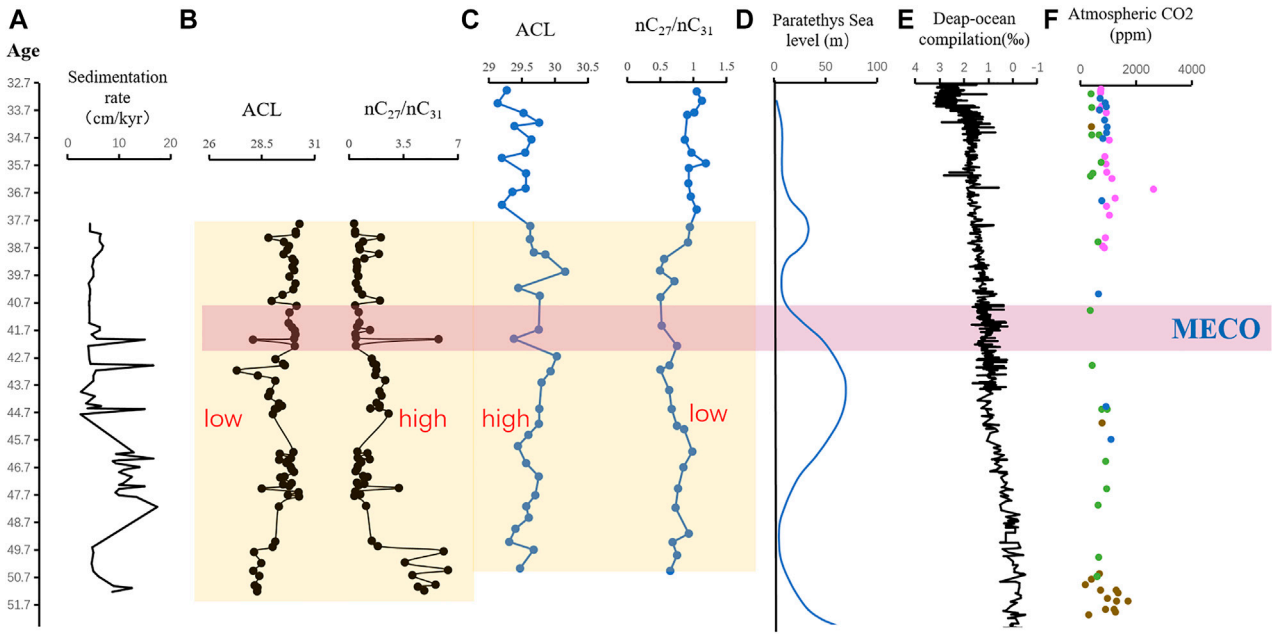

FIGURE 5
(A) Sedimentation rate in this study. **(B)** The *n*-alkane data was obtained in this study. **(C)** The *n*-alkane results were made by the predecessors in the Xining Basin (Long et al., 2011). **(D)** The retreat process of the Tethys Sea (Sun et al., 2016). **(E)** The Eocene global deep-sea oxygen isotope changes (Zachos et al., 2001). **(F)** Global atmospheric CO_2 concentration since the Cenozoic (Steinthorsdottir et al., 2019).

nC_{31} indicates the evolution of herbaceous plants to woody plants, and the decrease in nC_{27}/nC_{31} indicates the evolution of woody plants to herbaceous plants (Xie et al., 1999). Different chain lengths correspond to the different plant sources; therefore, the average carbon chain lengths (ACL) of long-chain alkanes (carbon number > nC_{26}) from lake sediments can also be used to indicate different vegetation types (Xie et al., 1999). The ACL of herbaceous plants is greater than the woody plants(; Liu et al., 2018) and the ACL value change can reflect the change in the relative abundance of woody and herbaceous plants.

The carbon isotopic composition of leaf paraffin hydrocarbons is commonly used to indicate paleovegetation types (Garcin et al., 2014; Niedermeyer et al., 2017) and paleoecological environment changes (wu et al., 2019b) and has also been applied by some scholars in the paleoelevation reconstruction of the Qinghai–Tibet Plateau (Deng and Jia, 2018; Sun et al., 2015).

As for the emergence time of C_3 and C_4 plants, many previous studies have been carried out. Existing evidence shows that C_4 plants mainly appeared in Miocene around 23 Ma, the earliest to Oligocene about 32 Ma according to the sharp decline in atmospheric CO_2 concentration (Vicentini et al., 2008; Hackel et al., 2018; Bouchenak et al., 2010). So in this study, the latest deposition age of the Nangqian Basin section is around 35 Ma. Also, the growth environment of C_4 plants is in the low–mid latitude region at a lower altitude (Boutton et al., 1980). Although C_4 plants can also be seen on the Qinghai–Tibet plateau, the biomass proportion is very low (Deng and Li,2005). According to previous studies, the altitude of the Nangqian Basin in the Eocene reached 3000 m (Fang et al., 2020). Thus, before 35 Ma, existing evidence showed that there was hardly a large number of C_4 plants, so the source of Eocene sediments in the Nangqian Basin was mainly C_3 plants.

The nC_{27}/nC_{31} value and ACL value (carbon nC_{27}-nC_{33}) of the sediments from the Nangqian section showed some correlation (n=67, R^2=0.47), According to the nC_{27}/nC_{31} values, ACL and CPI values and the variation characteristics of carbon isotope $\delta^{13}C$ of *n*-alkanes, the evolution of palaeovegetation in the Nangqian section can be divided into three stages, which are relatively consistent with the changes of sedimentary facies.

Stage I: 51.8–46.4 Ma, the main plant types were mid-chain woody aquatic plants. In this period, the depositional environments consisted of a braided river and an ephemeral lake, and the fluvial sedimentary facies were an open system with strong hydrodynamic conditions. In this system, the terrestrial plants carried by surface runoff may be an important factor affecting the input of terrestrial plants. Therefore, the phenomenon of high overall chain length shown by ACL and nC_{27}/nC_{31} in this period may be caused by the input of exogenous terrestrial vegetation brought by rainfall and surface runoff.

Stage II: 46.4–42.7 Ma, during which the depositional environments gradually became stable and changed from braided rivers and ephemeral lakes to brackish lakes. As for compound-specific carbon isotope $\delta^{13}C$ of *n*-alkanes, the value of $\delta^{13}C$ of *n*-alkanes gradually showed a positive trend. At the same time, ACL values gradually increased, while nC_{27}/nC_{31} gradually decreased, the Paq value decreased significantly, and the main carbon number gradually changed to a high carbon number, most of which was nC_{25}, indicating that the overall vegetation type changed from woody plants to herbaceous plants in this period. The TOC also increased significantly compared with the previous stage, indicating that plant productivity increased with the stable sedimentary environment.

Stage III: 42.7–37.5 Ma, in this period, the depositional environments mainly consisted of mudflats and salt lakes. In terms of *n*-alkanes, the ACL value kept a low trend and the CPI value increased significantly, while the Paq value and nC_{27}/nC_{31} value also kept a low value on the whole. The proportion of high carbon number in main peak carbon increased significantly, indicating a rapid change in the proportion of terrestrial higher plants. With the further stability of the sedimentary environment, TOC content also increased further. In summary, herbaceous plants were still the main vegetation type in this period.

5.3 Paleoclimatic evolution

Previous studies have shown that the Paq value, the relative input index of *n*-alkanes of aquatic plants, can reflect the change in precipitation in geological history. A higher Paq value indicates a higher content of mid-chain *n*-alkanes from submerged/floating plants, indicating the expansion of the lake and higher humidity. On the contrary, the contribution of terrigenous higher plants and emergent plants increased, indicating low lake surface and relatively arid climate conditions. Relevant research conclusions have been confirmed and widely applied to the Qinghai–Tibet Plateau (Cranwell, 1973; Pu et al., 2011; Duan and Xu, 2012; Zheng et al., 2007; Cui et al., 2008). In addition, Eglinton and Hamilton considered that temperature is positively correlated with *n*-alkanes chain length (ACL). Plants tend to synthesize longer chains of *n*-alkanes when temperature increases (Eglinton and Hamilton, 1967). At the same time, Poynter and Eglinton proposed that the change of ACL value could reflect the relative change of paleotemperature in marine sediments and believed that the change of ACL value could reflect the relative change of paleotemperature in the source area of terrestrial sediments. The research results were also confirmed in the study of *n*-alkanes and temperature changes in modern plant leaves (Sorrel et al., 2017; He et al., 2018).

In addition, the carbon isotope of leaf paraffin in sediments is related to the types of vegetation photosynthesis, atmospheric CO_2 isotope and CO_2 concentration, temperature, precipitation, and other factors in the sedimentary basin.

Leaf paraffin alkane is formed by photosynthesis through the absorption of atmospheric CO_2 by plants. Therefore, the carbon isotopic composition of a single alkane is related to atmospheric CO_2 isotopic composition. However, the variation range of atmospheric CO_2 isotope was less than 0.8‰ during the Eocene (Tipple, 2010). Assuming that the degree of fractionation between vegetation and atmospheric CO_2 did not change, the variation of carbon isotope of CO_2 could only cause the variation of carbon isotope of leaf alkane to less than 0.8‰. In the Nangqian Basin, the variation range of a single carbon isotope can reach more than 10‰, which indicates that the single carbon isotope in the Nangqian Basin may be affected by atmospheric CO_2 isotope variation to some extent, but it is not important.

At the same time, the reduction of the atmospheric CO_2 concentration will reduce the degree of carbon isotope fractionation between leaf paraffin and atmospheric CO_2 and then affect the plant leaf paraffin isotope (Schubert and Jahren, 2012). However, the resolution of the study on the change in atmospheric CO_2 concentration is low and controversial. According to the available data, the global cooling of EOGM (Earliest Oligocene Glacial Maximum) events in the late Eocene may be related to the decrease in atmospheric CO_2 concentration (Barron, 1985; Pearson et al., 2009). If the alkane isotopes of leaf wax were mainly affected by the change of atmospheric CO_2 concentration in the Eocene, the carbon isotopes should show the same trend as atmospheric CO_2 concentration in the Eocene. However, the carbon isotope of the Nangqian Basin showed a positive deviation with the passage of time during the Eocene, which did not correspond well with the change of atmospheric CO_2 concentration, indicating that the change of atmospheric CO_2 concentration was not the main factor affecting the change of carbon isotope of *n*-alkanes.

Pollen fossil studies show that the vegetation of the YAL section (41–40 Ma) in the Nangqian Basin is dominated by mixed pollen of angiosperms and gymnosperms, of which the angiosperms are dominated by Nitraria and gymnosperms by Ephedra and Taxaceae (Yuan et al., 2016). In the RZ section, the dominant vegetation types of the Nangqian Basin did not change much in the late Eocene (41–38 Ma). Different types of plants have different carbon isotopes, *n*-alkanes in pine and cypress plants are more enriched in ^{13}C than angiosperms. (Diefendorf and Freimuth, 2016; Pedentchouk et al., 2008). Therefore, if the coniferous and cypress plants increase in the basin, the carbon isotope of middle paraffin in river and lake sediments will increase. By comparing the carbon isotopes of *n*-alkanes from the late Eocene in the Nangqian Basin, it was found that the carbon isotopes of leaf paraffin were positively skewed with the decrease of coniferous and cypress gymnosperms, indicating that the change in vegetation type was not the direct factor causing the change of carbon isotopes of *n*-alkanes. The climatic factors

leading to the change of vegetation types may be the main reason for the change of compound-specific carbon isotopes.

Recent studies on carbon isotopic compositions of plants at a global scale show that the carbon isotopic compositions of organic matter and *n*-alkanes in leaves of modern plants are obviously influenced by environmental factors, especially by annual average precipitation. A previous study (Diefendorf et al., 2010) summarized the carbon isotope data of 3310 leaves of 557 species of trees from 105 sampling sites around the world, revealing that there was a significant positive correlation between the carbon isotope fractionation among leaves of atmospheric CO_2 and the annual average precipitation, indicating that in a large spatial range, the regulation of leaf stomata on CO_2 exchange caused by water balance pressure is the main mechanism affecting carbon isotope fractionation in plants. Similarly, previous research (Kohn, 2010) collected carbon isotope data of C3 plants from 570 published sampling sites around the world and found that the carbon isotope of C_3 plants decreased with the increase in annual average precipitation. Most of the plants whose $\delta^{13}C$>-25.5‰ distributed in the region with annual mean precipitation less than 500mm, and the correlation between plant carbon isotope and precipitation gradually weakened when annual mean precipitation exceeded 1,000 mm. Liu and An (2020) collected and collated carbon isotopes of leaf paraffin from major plant types around the world and found that there is a significant negative correlation between carbon isotopes of *n*-alkanes from C3 plants and annual average precipitation, but a weak correlation between carbon isotopes and annual average temperature. However, carbon isotopes of leaf paraffin in C4 plants and monocotyledon plants have a weak correlation with annual average precipitation and an obvious positive correlation with annual average temperature. Therefore, the author believes that, on the basis of clear paleovegetation types, carbon isotopes of leaf paraffin can be used in the study of paleoprecipitation and paleotemperature. The vegetation types of the Nangqian Basin from the Eocene were dominated by C3 plants. Therefore, carbon isotopes of leaf paraffin may indicate the variation of annual average precipitation in the basin.

According to the results of this study, during the period of 51.8–37.5 Ma, the overall variation trend of *n*-alkanes in the Nangqian profile is relatively consistent (Figure 4), indicating that vegetation in the Nangqian Basin is sensitive to climate change, especially in terms of temperature and humidity. According to the index including the TOC, *n*-alkanes, and carbon isotope change trend in the Nangqian profile, there were obvious climate shifts at 46.4 and 42.7 Ma, which accord with the change of sedimentary facies; accordingly, the paleoclimate evolution of the Nangqian Basin from the Eocene to Oligocene can be divided into the following three stages.

Stage I: 51.8–46.4 Ma, the sedimentary facies were a braided river and an ephemeral lake, which suggests that this period kept relatively humid climate conditions; meanwhile, the carbon isotope $\delta^{13}C$ of *n*-alkanes is generally negative, indicating a relatively humid sedimentary environment.

Previous studies on the chain length distribution characteristics of leaf paraffin of various plant types in 400 mm precipitation line in China showed that temperature in the summer (growing season) has an important influence on the chain length distribution of leaf paraffin in terrestrial higher plants. The higher the temperature in summer, the greater the ACL, but the change of ACL can only be a qualitative indicator of temperature change. It cannot be used as a quantitative indicator of temperature (Wang et al., 2018). However, such a conclusion also needs a stable sedimentary environment and vegetation type as the foundation support. In stage I, the sedimentary facies consisted of fluvial facies and ephemeral lake facies, which were relatively unstable on the whole. ACL was not an accurate indicator to reflect the trend of temperature change. At this stage, TOC has a reflection of the organic matter content in lake sediments and also has a relatively low value, it may also be affected by the unstable sedimentary environment and influenced the preservation of organic matter; therefore in stage Ⅰ period, the Nangqian Basin temperature change may need more evidence to explore further.

Stage Ⅱ: 46.4–42.7 Ma. In this stage, the ACL values of the samples increased significantly, while nC_{27}/nC_{31} and Paq values decreased. Indicating climate dry trends because the ACL of plant leaf paraffin reflects the leaf epidermis of epicuticular wax on leaf water balance degree, the longer the carbon chain lock water ability, the stronger ACL exists in correlation with the temperature because of blades on the regulation of water in plants, and as the temperature increases, leaf transpiration of water also increases. In order to maintain water balance in the body, the upper epidermis of leaves needs to be more water-locked, so the carbon chain of leaf paraffin synthesized by plants is longer (Wang et al., 2018). Thus, in a relatively stable sedimentary environment, ACL values rise and Paq value decreases indicating a long-term climate drying trend gradually. As for temperature changes in this period, under the background of the overall global cooling, the ACL index cannot separately be used to measure temperature change; concrete temperature changes still need further discussion. During this period, the vegetation type changed greatly, from woody to herbaceous, in response to the climate characteristics of drying.

Stage Ⅲ: 42.7–37.5 Ma, during this period, nC_{27}/nC_{31} and Paq values remain low, while ACL values remain high. As can be seen from the distribution characteristics of *n*-alkanes in this study, odd–even dominance is mainly concentrated in the range of high carbon numbers; accordingly, it may mean that the

productivity of higher plant vegetation is significantly improved, as shown in Fig. 4.1, from 42.7 to 37.5 Ma, the distribution of NQ 1 segment samples gradually changed from unimodal to bimodal. In addition, compared with stage II, the sedimentary environment of stage III changed but was still stable. According to lithology, redox conditions were slightly elevated, but it is generally believed more reductive sedimentary environment is more suitable for the preservation of organic matter; thus, as for TOC changes, the preservation condition may not be the main factor. TOC increased during this period. It indicates that the climatic conditions became more suitable for herbaceous plants during this stage. ACL values also maintained high values in a relatively stable sedimentary environment, which may be some response to the temperature warming and correspond well to the Middle Eocene Climatic Optimum (MECO) event at around 40 Ma in the same period. They may be influenced by the MECO, the carbon isotope $\delta^{13}C$ of *n*-alkanes was significantly positive in the whole during this period, indicating that climatic conditions had turned noticeably drier.

It was previously believed that a lower ratio of Pr/Ph (Pr/Ph < 0.6) usually represents a hypersaline environment of hypoxia, while a higher gammacerane also reflects higher environmental salinity Peters and Moldowen, 1993. We calculated the average values of Pr/Ph among the three different stages (Table 1) and found that the average value of Pr/Ph in stage I is 0.30, stage II is 0.38, and stage III is 0.31, showing a certain increasing trend. Similarly, the maximum value of G/nC_{30}H was 2.19 and the minimum value was 0.006. The average value was 0.26, and the average value was 0.02 in stage I, 0.13 in stage II, and 0.43 in stage III, during the whole 51.8–37.5 Ma period, the gammacerane increased generally and decreased in the late stage, which may be caused by the weakening of water stratification caused by the change of sedimentary environment. Therefore, the overall salinity of the Nangqian Basin also gradually increases during the whole long 51.8–37.5 Ma period. In particular, there is a relatively more obvious increase in salinity in stage III, which corresponds to the changes in sedimentary facies and the obvious increase of gypsum layers in outcrops, indicating that the overall climate characteristics of stage III are still drying.

Furthermore, the abovementioned compounds, especially Paq, showed some fluctuations during this period, which was consistent with the previous palynological results and clay mineral analysis results from the YAL profile, RZ profile in the Nangqian Basin, and Gongjue Basin dating from about 41.2 to 37.8 Ma (Bartonian Period) (Long et al., 2011; Miao et al., 2016; Yuan et al., 2016; Yuan et al., 2020). It was also consistent with the Eocene records of the Xining Basin (Figure 5), Qaidam Basin, and Hoh Xil Basin during the same period. Therefore, we believe that even under the condition of short-term warming and continuous drought, there was still short-term dry and wet alternation in this stage.

6 Driving mechanisms

The uplift of the Qinghai–Tibet Plateau is the most important tectonic event during the Cenozoic, mainly formed during the northward movement of the Indian plate and subsequent collision with the Eurasian plate. There are two views on the uplifting process of the Qinghai–Tibet Plateau. One view is that the Qinghai–Tibet Plateau has been gradually uplifted from south to north since the Eocene (Tapponnier, 2001). According to another view, the central Qinghai–Tibet Plateau rose to 3000–4000 m from the beginning of the Eocene (Wang et al., 2008), followed by the further compression and collision of the Indo-Asian plate and the southern Qinghai–Tibet Plateau gradually rose to its present height (Hatzfeld and Mohar, 2010). The northern Qinghai–Tibet Plateau (Hatzfeld and Mohar, 2010) and its surrounding mountains, such as the Tian Shan and the Pamir Mountains, were significantly uplifted after the Miocene. Despite the lack of consensus on the uplifting history of the Qinghai–Tibet Plateau, both views indicate that the uplifting of the Qinghai–Tibet Plateau was a multi-stage, multi-act process since the Eocene. The uplift of the Qinghai–Tibet Plateau plays an important role in global and regional climate change, many previous simulations, with or without the Qinghai–Tibet Plateau as the main body, have found that uplifting processes affect the formation and evolution of the Asian monsoon (Manabe and Terpstra, 1974), aridity in the Asian interior (Kutzbach et al., 1993; Manabe and Broccoli, 1990; Broccoli and Manabe., 1992), and regional and global climate change (Kutzbach et al., 1989; Kutzbach et al., 1993; Ruddiman and Kutzbach., 1991).

During the Eocene, one of the important sources of water vapor in the Qinghai–Tibet Plateau was the Paratethys Sea. The change of the Paratethys Sea can lead to a change in the thermal properties between the sea and land. Therefore, the retreat of the Paratethys Sea means that the water vapor leading to the Qinghai–Tibet Plateau decreases and its influence on the process of aridity is obvious. From the late Eocene to the Early Oligocene, the Indian plate and the Asian plate collided constantly, and the decrease in sea level during the same period indicates the further disappearance of the Paratethys Sea. The water vapor source in the inland area of the Qinghai–Tibet Plateau is mainly controlled by the westerly circulation; therefore, the retreat of the Paratethys Sea must have a necessary impact on the aridification process in the inland area of the Qinghai–Tibet Plateau.

In this study, by comparing the climate evolution characteristics recorded by *n*-alkane-related indexes and TOC in the Nangqian Basin with that recorded in the Xining Basin (Long et al., 2011) (Figure 5), it can be found that during the period of 50.5–37.8 Ma, vegetation types in the Xining Basin gradually evolved from woody plants to herbaceous plants and the climate was dry and warm, which had similar evolutionary characteristics with the Nangqian Basin. The results of previous studies on the Shuiwan section of the Xining Basin during the

Eocene showed that the grain size characteristics of mudstone samples were very similar to the grain size characteristics of loess in the Yili Basin and were also subject to the west risk control (Long et al., 2011; Wang et al., 2014).

Numerous climate simulation experiments and numerical studies indicate that more than 60% of the water reaching Central Asia today is transported by the westerlies (Yatagai and Yasunari, 1998; Numaguti, 1999; Sato et al., 2007); the westerlies may dominate the overall water budget of the Qinghai–Tibet Plateau (Curio et al., 2015). In the study of the geological record of the younger, the westerly played a leading role in water vapor transport. During the entire Holocene period, western central Asia (Caspian sea to east Kazakhstan) and central Asia (northwest China to eastern Mongolia) drought indexes are synchronized and show a negative correlation between the change of the monsoon moisture index and drought index (Chen et al., 2010), indicating that during this period, the transport of water vapor by westerly winds controlled the drought in most parts of Eurasia. In addition, GCM (General Circulation Model) with paleoboundary conditions indicates that westerly winds also played an important role in controlling the Cenozoic climate in Central Asia (Ramstein et al., 1997; Zhang et al., 2007; Huber and Goldner, 2012).

According to the oxygen isotope records of paleosoil carbonate in the Mongolian Plateau (Caves et al., 2015), more than 2,650 paleosoil and lacustrine carbonate data points across Asia, and modern precipitation data, indicating that the spatial distribution of paleoprecipitation in the whole Asia is highly similar to that in modern times. (Caves et al., 2015; Bougeois et al., 2018). In this study, the depositional rate of the Nangqian Basin in the Eocene was calculated, and the results showed that the depositional rate in the early and middle Eocene was significantly higher than that in the middle and late Eocene, which may mean that the uplift degree of the Nangqian Basin in the early and middle Eocene was greater than that in the middle and late Eocene. Therefore, the plateau uplift may have had little influence on the water vapor transport path to the Nangqian Basin during the middle and late Eocene. Thus, we consider that the driving mechanism of Eocene climate change in the Nangqian Basin is similar to that in the Xining Basin, and the source of water vapor is consistent, which is mainly controlled by westerly winds.

Previous studies on oxygen isotopes of carbonate in the Nangqian Basin (Hasty, 2011) and paleoelevation of the Lunpola Basin in the middle of the Qinghai–Tibet Plateau (Wei et al., 2017) showed that the altitude of the Qinghai–Tibet Plateau increased during the Eocene, combined with the uplift and compression of the Pamir tectonic belt, this may further lead to the retreat of the Paratethys Sea during 47.0–40.0 Ma (Sun et al., 2016). Meanwhile, the climate of the Nangqian Basin also showed continuous aridification. In addition, the global deep-sea oxygen isotope decreased during the middle and late Eocene, while the global atmospheric CO_2 concentration increased during the same period, indicating that the global climate cooled significantly during this period, which may have made the water vapor transport in inland areas more difficult. Furthermore, previous studies have shown that one of the main causes of Asian inland aridity may also be global climate cooling. For example, Long et al. (2011) studied sediments in Xining Basin by combining *n*-alkanes biomarkers and palynological records. It is believed that the cooling and drying of climate during the period from the end of the Eocene to the beginning of the Oligocene was caused by the decline of global temperature during this period, which is consistent with the conclusion of Dupont (2007, 2008). The water vapor transport in the Nangqian Basin during the Eocene was mainly controlled by the westerlies, so the Paratethys Sea provides the largest water vapor source; therefore, the Paratethys Sea retreat and global climate cooling may jointly lead to the climate aridity in the Nangqian Basin.

In addition, the uplift of the Qinghai–Tibet Plateau may further block the influence of the South Asian monsoon on the central and eastern Qinghai–Tibet Plateau, so that the water vapor carried by the South Asian monsoon cannot reach the inland area of the Qinghai–Tibet Plateau. A total of three hypotheses have been proposed to explain the increasing aridity in Central Asia since the Cenozoic by using sedimentary records and the general circulation model (GCM) to study the relationship between topography and climate. The first hypothesis holds that the staged uplift of the Qinghai–Tibet Plateau blocked water vapor from the south, and the lower temperature on the plateau exacerbated the atmospheric subsidence, further leading to Cenozoic droughts in Central Asia (Kutzbach et al., 1993; An et al., 2001; Sato and Kimura., 2005; Zhang et al., 2007; Sato, 2009). Both the second and third hypotheses are based on the correlation between aridification and global climate change and believe that global climate plays a leading role in accelerating the evolution of drought in Central Asia but have different views on the driving mechanism influencing the aridification in Central Asia (Abels et al., 2011; Bosboom et al., 2014; Dupont-nivert et al., 2007; Miao et al., 2013; Song et al., 2014). It has been suggested that the gradual westward retreat of the Paratethys Sea and the global cooling of the Cenozoic may have reduced the water vapor source from the westerlies in the past 50 Ma, then leading to aridification (Bosboom et al., 2014; Miao et al., 2012). Another view is that the decline of monsoon intensity in the Cenozoic may be one of the reasons for the intensification of drought in Central Asia (Licht et al., 2014).

In contrast, during the middle–late Eocene, there exists obvious differences in depositional environment between the Nangqian Basin and other regions including southeastern (Sorrel et al., 2017; Su et al., 2019) (Jianchuan Basin and Markam Basin) and southwestern (Lunpola Basin) (Wei et al., 2017) part of the Qinghai–Tibet Plateau, these basins mainly represent the rivers, swamps, delta, and lake environment, but the Nangqian Basin is

mainly salt lake facies. In these basins, fossil plants are abundant, especially found in the obvious formation of coal in the Jianchuan Basin, this suggests that the more humid climate conditions in southern Tibet, may be explained by a tropical/subtropical climate, driven by I ~ AM (Indonesia to Australian monsoon) from the south monsoon (Spicer, 2017). This is in sharp contrast to the semi-arid/arid climate in the north and northeast of Central Tibet (Nangqian Basin, Xining Basin, Qaidam Basin, etc.). Therefore, we believe that the Nangqian Basin was less affected by the southern monsoon during the Eocene.

7 Conclusion

In this study, we reconstructed the paleoclimate and paleovegetation evolution history from 51.8 Ma to 37.5 Ma in the central and eastern Qinghai–Tibet Plateau by comparing the *n*-alkane-induced indices, the carbon isotope $\delta^{13}C$ of *n*-alkanes, and the total organic carbon content of the sediments from the Nangqian section and reached the following preliminary conclusions:

1) The source of organic matter in the Nangqian Basin is mainly submerged floating aquatic plants, while some terrigenous higher plants are imported, and fungi, algae, and aquatic low implanting inputs are less.
2) According to the indexes of organic geochemistry, the evolution of paleoclimate and paleovegetation in the Nangqian Basin from 51.8–37.5 Ma can be divided into three stages: stage I: 51.8–46.4 Ma, the climate was humid, and the vegetation type was mainly aquatic herbaceous plants. Stage II: 45.0–42.7 Ma, the climatic conditions showed gradual droughts, accompanied by periodic drought and wet changes; the vegetation type changed from woody plants to herbaceous plants. Stage III: 42.7–37.5 Ma, the climatic conditions continued to be dry, which may have been affected by the MECO events, and the content of organic matter obviously increased; the vegetation type was mainly herbaceous plants.
3) Through the comparative study of the climate evolution history of the Eocene in the Nangqian Basin reconstructed by the multi-index system with the climate change in the adjacent area, the retreat process of the proto-Paratethys Sea, the global deep-sea oxygen isotopes, and the global atmospheric CO_2 concentration, it is considered that the Eocene climate change in the Nangqian Basin is mainly affected by the global climate change and the retreat of the proto-Paratethys Sea. The uplift of the Qinghai–Tibet Plateau and the increase of altitude have little influence on the water vapor in the Nangqian Basin, while the basin was less affected by the South Asian monsoon (Walker et al., 1981; Berner et al., 1983; Ruddiman and Kutzbach, 1989; Raymo and Ruddiman, 1992; Molnar et al., 1993; Sage, 2001; Deng and LI, 2005; Zachos and Kump, 2005; Wang, 2006; Bouchenak-Khelladi et al., 2009; Hren et al., 2009; Yang et al., 2011a; Yang et al., 2011b; Hou et al., 2017; Dupont-Nivet et al., 2018; Lin et al., 2018; Xu et al., 2019; Ye et al., 2020).

Data availability statement

The original contributions presented in the study are included in the article/Supplementary Material; further inquiries can be directed to the corresponding author.

Author contributions

The main author of this manuscript is SL. ZW, YW, GW, TZ, and XM have put forward a lot of valuable suggestions and assisted in the modification of the manuscript. XY, WH, PZ, HM, and JW have all participated in the experimental process and made contributions.

Funding

This work was financially supported by the Second Qinghai–Tibet Plateau Scientific Expedition and Research (STEP) Program (Grant No. 2019QZKK0707), the National Key R&D Program of China (Grant No. 2017YFA0604803), the Chinese Academy of Sciences Key Project (Grant No. XDB26020302), the National Natural Science Foundation of China (Grant Nos. 41831176, 41902028, and 41972030), and the CAS "Light of West China" Program and the Key Laboratory Project of Gansu (Grant No. 1309RTSA041).

Conflict of interest

The authors declare that the research was conducted in the absence of any commercial or financial relationships that could be construed as a potential conflict of interest.

Publisher's note

All claims expressed in this article are solely those of the authors and do not necessarily represent those of their affiliated organizations, or those of the publisher, the editors, and the reviewers. Any product that may be evaluated in this article, or claim that may be made by its manufacturer, is not guaranteed or endorsed by the publisher.

References

Abels, H. A., Dupont-Nivet, G., Xiao, G. Q., Bosboom, R., and Krijgsman, W. (2011). Step-wise change of asian interior climate preceding the eocene–oligocene transition (EOT). *Palaeogeogr. Palaeoclimatol. Palaeoecol.* 299 (3-4), 399–412. doi:10.1016/j.palaeo.2010.11.028

Aichner, B., Herzschuh, U., and Wilkes, H. (2010). Influence of aquatic macrophytes on the stable carbon isotopic signatures of sedimentary organic matter in lakes on the Tibetan Plateau. *Org. Geochem.* 41(7):706-718, doi:10.1016/j.orggeochem.2010.02.002

An, Z. S., Kutzbach, J. E., Prell, W. L., and Porter, S. C. (2001). Evolution of asian monsoons and phased uplift of the Himalaya~Qinghai-Tibet plateau since late Miocene times. *Nature* 411, 62–66. doi:10.1038/35075035

Barron, E. J. (1985). Explanations of the tertiary global cooling trend. *Palaeogeogr. Palaeoclimatol. Palaeoecol.* 50 (1), 45–61. doi:10.1016/s0031-0182(85)80005-5

Berner, R. A., Lasaga, A. C., and Garrels, R. M. (1983). The carbonate-silicate geochemical cycle and its effect on atmospheric carbon dioxide over the past 100 million years. *Am. J. Sci.* 283, 641–683. doi:10.2475/ajs.283.7.641

Bosboom, R., Dupont-Nivet, G., Grothe, A., Brinkhuis, H., Villa, G., Mandic, O., et al. (2014). Timing, cause and impact of the late Eocene stepwise sea retreat from the Tarim Basin (west China). *Palaeogeogr. Palaeoclimatol. Palaeoecol.* 403, 101-118, doi:10.1016/j.palaeo.2014.03.035

Bouchenak-Khelladi, Y., Verboom, G. A., Hodkinson, T. R., Salamin, N., Francois, O., Ni Chonghaile, G., et al. (2009). The origins and diversification of C4 grasses and savanna-adapted ungulates. *Glob. Chang. Biol.* 15 (10), 2397–2417. doi:10.1111/j.1365-2486.2009.01860.x

Bougeois, L., Dupont-Nivet, G., De Rafélis, M., Tindall, J. C., Proust, J. N., Reichart, G. J., et al. (2018). Asian monsoons and aridification response to Paleogene sea retreat and Neogene westerly shielding indicated by seasonality in Paratethys oysters. *Earth Planet. Sci. Lett.* 485, 99–110. doi:10.1016/j.epsl.2017.12.036

Boutton, T. W., Harrison, A. T., and Smith, B. N. (1980). Distribution of biomass of species differing in photosynthetic pathway along an altitudinal transect in southeastern Wyoming grassland. *Oecologia* 45 (3), 287–298. doi:10.1007/bf00540195

Broccoli, A., and Manabe, S. (1992). The effects of orography on midlatitude Northern Hemisphere dry climates. *J. Clim.* 5, 1181–1201, doi:10.1175/1520-0442(1992)005<1181:teooom>2.0.co;2

Caves, J. K., Winnick, M. J., Graham, S. A., Sjostrom, D. J., Mulch, A., and Chamberlain, C. P. (2015). Role of the westerlies in central Asia climate over the cenozoic. *Earth Planet. Sci. Lett.* 428, 33–43. doi:10.1016/j.epsl.2015.07.023

Chen, F., Chen, J., HolmesJBoomer, I., Austin, P., Gates, J. B., et al. (2010). Moisture changes over the last millennium in arid central Asia: A review, synthesis and comparison with monsoon region. *Quat. Sci. Rev.* 29, 1055–1068. doi:10.1016/j.quascirev.2010.01.005

Cranwell, P. A., Eblinton, G., and Robinson, N. (1987). Lipids of aquatc organisms as potential Contributors to lacustrine sediments[J]. *Org. Geochem* 11, 513–527. doi:10.1016/0146-6380(87)90007-6

Cranwell, P. A. (1973). Chain-length distribution of n-alkanes from lake sediments in relation to post-glacial environmental change. *Freshw. Biol.* 3 (3), 259–265. doi:10.1111/j.1365-2427.1973.tb00921.x

Cui, J., Huang, J., and Xie, S. (2008). Seasonal changes of leaf alkanes and olefins in Qingjiangmodern plant, HubeiProvince[J]. *Chin. Sci. Bull.* 53 (11), 1318–1323. doi:10.1007/s11434-008-0194-8

Curio, J., Maussion, F., and Scherer, D. A. (2015). A 12-year high-resolution climatology of atmospheric water transport over the Tibetan Plateau. *Earth Syst. Dyn.* 6, 109–124. doi:10.5194/esd-6-109-2015

Damsté, S., and Jaap, S. (2012). A 25,000-year record of climate-driven vegetation change in the lowland savanna of eastern equatorial Africa revealed by the carbon-isotopic signature of fossil plant leaf waxes[J]. *Quat. Int.* 279–280, 453.

Deng, L., and Jia, G. (2018). High-relief topography of the Nima basin in central Tibetan Plateau during the mid-Cenozoic time. *Chem. Geol.* 493, 199–209, doi:10.1016/j.chemgeo.2018.05.041

Deng, T., and Li, Y. (2005). Vegetational ecotype of the Gyirong Basin in Tibet, China and its response in stable carbon isotopes of mammal tooth enamel. *Chin. Sci. Bull.* 50, 1225–1229. doi:10.1360/04wd0275

Diefendorf, A. F., and Freimuth, E. J. (2016). Extracting the most from terrestrial plant-derived n-alkyl lipids and their carbon isotopes from the sedimentary record: A review[J]. *Org. Geochem.*, 1–21. doi:10.1016/j.orggeochem.2016.10.016

Diefendorf, A, F., Mueller, K. E., Wing, S. L., and Freeman, K. H. (2010). Global patterns in leaf 13C discrimination and implications for studies of past and future climate[J]. *Proc. Natl. Acad. Sci.* 107, 5738–5743. doi:10.1073/pnas.0910513107

Dodd, R. S., and Afzal-Rafii, Z. (2000). HABITAT-RELATED adaptive properties of plant cuticular lipids[j]. *Evolution* 54 (4), 1438. doi:10.1554/0014-3820(2000)054[1438:HRAPOP]2.0.CO;2

Duan, Y., and Xu, L. (2012). Distributions of n-alkanes and their hydrogen isotopic composition in plants from Lake Qinghai(China) and the surrounding area. *Appl. Geochem.* 27 (27), 806–814. doi:10.1016/j.apgeochem.2011.12.008

Dupont-nivet, G., Krijgsman, W., Langereis, C. G., Abels, H. A., Dai, S., and Fang, X. (2007). Tibetan plateau aridification linked to global cooling at the Eocene–Oligocene transition. *Nature* 445 (7128), 635–638. doi:10.1038/nature05516

Dupont-Nivet, G., Dai, S., Fang, X. M., Erens, V., Krijgsman, W., Reitsma, M., et al. (2018). Timing and distribution of tectonic rotations in the northeastern Tibetan Plateau [J]. *Geol. Soc. Am. Special Pap.* 444, 73–87. doi:10.1130/2008.2444(05)

Edmond, J. M. (1992). Himalayan tectonics, weathering processes and the strontium isotope record in marine limestones. *Science* 258, 1594–1597. doi:10.1126/science.258.5088.1594

Eglinton, G., and Hamilton, R. J. (1967). Leaf epicuticular waxes. *Science* 156 (3780), 1322–1335. doi:10.1126/science.156.3780.1322

Fang, X., Dupont-Nivet, G., Wang, C., Song, C., Meng, Q., Zhang, W., et al. (2020). Revised chronology of central Tibet uplift (Lunpola basin). *Sci. Adv.* 6 (50), eaba7298. doi:10.1126/sciadv.aba7298

Fang, X. M., Guo, Z. T., Jiang, D. B., and Spicer, R. A. (2021). No monsoon-dominated climate in subtropical Asia before 35 Ma. *Sci. Adv.* Accepted.

Ficken, K. J., Li, B., Swain, D. L., and Eglinton, G. (2000). An n-alkane proxy for the sedimentary input of submerged/floating freshwater aquatic macrophytes. *Org. Geochem.* 31 (7), 745–749. doi:10.1016/s0146-6380(00)00081-4

Fielding, E., Isacks, B., Barazangi, M., and Duncan, C. (1994). How flat is Tibet? *Geol.* 22, 163–167. doi:10.1130/0091-7613(1994)022<0163:hfit>2.3.co;2

Garcin, Y., Schefu?, E., Schwab, V. F., Garreta, V., Gleixner, G., and Vincens, A. (2014). Reconstructing C3 and C4 vegetation cover using n-alkane carbon isotope ratios in recent lake sediments from Cameroon, Western Central Africa. *Geochimica. Et. Cosmochimica Acta.* 142:482-500, doi:10.1016/j.gca.2014.07.004

Hackel, J., Vorontsova, M., Nanjarisoa, O. P., Hall, R. C., Razanatsoa, J., Malakasi, P., et al. (2018). Grass diversification in Madagascar: *In situ* radiation of two large C_3 shade clades and support for a Miocene to pliocene origin of C_4 grassy biomes. *J. Biogeogr.* 45 (4), 750–761. doi:10.1111/jbi.13147

Harris, N. B. W. (2006). The elevation history of the Tibetan Plateau and its implications for the Asian monsoon. *Palaeogeogr. Palaeoclimatol. Palaeoecol.* 241, 4–15. doi:10.1016/j.palaeo.2006.07.009

Hasty, S. (2011). New biomedical engineering study findings have been reported by researchers at university of miami, department of biomedical engineering[J]. *Energy Bus. J.*, 11–12.

Hatzfeld, D., and Molnar, P. (2010). Comparisons of the kinematics and deep structures of the Zagros and Himalaya and of the Iranian and Tibetan plateaus and geodynamic implications. *Rev. Geophys.* 48 (2), RG2005. doi:10.1029/2009rg000304

He, W., Wang, G., Wang, Y., Wei, Z., Gong, J., Zhang, T., et al. (2018). The characteristics of paleoclimate environment over the past 30 cal kaB.P. recorded in lacustrine depositsof the Qionghai Lake, Sichuan Province [J]. *Quat. Res.* 38 (5), 1179–1192. doi:10.11928/j.issn.1001-7410.2018.05.12

Horton, B. K., Yin, A., Spurlin, M. S., Zhou, J., and Wang, J. (2002). Paleocene-Eocene syncontractional sedimentation in narrow, lacustrine-dominated basins of east central Tibet. *Geol. Soc. Am. Bull.* 114, 771–786. doi:10.1130/0016-7606(2002)114<0771:pessin>2.0.co;2

Hou, J., D'Andrea William, J., Wang, M., He, Y., and Liang, J. (2017). Influence of the Indian monsoon and the subtropical jet on climate change on the Tibetan Plateau since the late Pleistocene. *Quat. Sci. Rev.* 163, 84–94. doi:10.1016/j.quascirev.2017.03.013

Hren, M. T., Bookhagen, B., Blisniuk, P. M., Booth, A. L., and Chamberlain, C. P. (2009). δ18O and δD of streamwaters across the Himalaya and Tibetan Plateau: Implications for moisture sources and paleoelevation reconstructions. *Earth Planet. Sci. Lett.* 288, 20–32. doi:10.1016/j.epsl.2009.08.041

Huber, M., and Goldner, A. (2012). Eocene monsoons. *J. Asian Earth Sci.* 44, 3–23. doi:10.1016/j.jseaes.2011.09.014

Kohn, M. J. (2010). Carbon isotope compositions of terrestrial C3 plants as indicators of (paleo)ecology and (paleo)climate. *Proc. Natl. Acad. Sci. U. S. A.* 107 (46), 19691–19695. doi:10.1073/pnas.1004933107

Kutzbach, J. E., Guetter, P. J., Ruddiman, W. F., and Prell, W. L. (1989). Sensitivity of climate to late Cenozoic uplift in southern Asia and the American west: Numerical experiments. *J. Geophys. Res.* 94 (D15), 18393–18407. doi:10.1029/jd094id15p18393

Kutzbach, J. E., Prell, W. L., and Ruddiman, W. F. (1993). Sensitivity of eurasian climate to surface uplift of the Tibetan plateau. *J. Geol.* 101 (2), 177–190. doi:10.1086/648215

Licht, A., Cappelle, M., Abels, H. A., Ladant, J. B., Donnadieu, Y., Vandenberghe, J., et al. (2014). Asian monsoons in a late Eocene greenhouse world[J]. *Nature* 513 (7519), 501–506. doi:10.1038/nature13704

Lin, L., Fan, M., Davila, N., Jesmok, G., Mitsunaga, B., Tripati, A., et al. (2018). Carbonate stable and clumped isotopic evidence for late Eocene moderate to high elevation of the east-central Qinghai-Tibet Plateau and its geodynamic implications [J]. *Geol. Soc. Am. Bull.* 131, 831–844. doi:10.1130/B32060.1

Liu, J., and An, Z. (2020). Leaf wax n-alkane carbon isotope values vary among major terrestrial plant groups: Different responses to precipitation amount and temperature, and implications for paleoenvironmental reconstruction. *Earth-Science Rev.* 202, 103081. doi:10.1016/j.earscirev.2020.103081

Liu, X., Cheng, Z., Yan, L., and Yin, Z. Y. (2009). Elevation dependency of recent and future minimum surface air temperature trends in the Tibetan Plateau and its surroundings. *Glob. Planet. Change* 68 (3), 164–174. doi:10.1016/j.gloplacha.2009.03.017

Long, L. Q., Fang, X. M., Miao, Y. F., Bai, Y., and Wang, Y. (2011). Northern Tibetan Plateau cooling and aridification linked to Cenozoic global cooling: Evidence from n-alkane distributions of Paleogene sedimentary sequences in the Xining Basin. *Chin. Sci. Bull.* 56 (15), 1569–1578. doi:10.1007/s11434-011-4469-0

Manabe, S., and Terpstra, T. B.. (1974). The Effects of Mountains on the General Circulation of the Atmosphere as Identified by Numerical Experiments. *J. Atmos. Sci.*, 31(1): 3-42, doi:10.1175/1520-0469(1974)031<0003:teomot>2.0.co;2

Manabe, S., and Broccoli, A. J. (1990). Mountains and arid climates of middle latitudes. *Science* 247 (4939), 192–195. doi:10.1126/science.247.4939.192

Miao, Y., Herrmann, M., Wu, F., Yan, X., and Yang, S. (2012). What controlled mid–late Miocene long-term aridification in central Asia? — global cooling or Tibetan plateau uplift: A review[J]. *Earth-Science Rev.* 112 (41702), 155–172. doi:10.1016/j.earscirev.2012.02.003

Miao, Y., Fang, X., Wu, F., Cai, M. T., Song, C. H., Meng, Q. Q., et al. (2013). Late cenozoic continuous aridification in the Western Qaidam Basin: Evidence from sporopollen records. *Clim. Past.* 9 (4), 1863–1877. doi:10.5194/cp-9-1863-2013

Miao, Y., Wu, F., Chang, H., Fang, X., Deng, T., Sun, J., et al. (2016). A Late-Eocene palynological record from the Hoh Xil Basin, northern Qinghai-Tibet Plateau, and its implications for stratigraphic age, paleoclimate and paleoelevation [J]. *Gondwana Res.* 31. doi:10.1016/j.gr.2015.01.007

Molnar, P., England, P., and Martinod, J. (1993). Mantle dynamics, uplift of the Tibetan plateau, and the Indian monsoon. *Rev. Geophys.* 31, 357–396. doi:10.1029/93rg02030

Molnar, P. (2005). Mio~Pliocene growth of the Qinghai-Tibet plateau and evolution of east asian climate. *Palaeontol. Electron* 8, 2–23.

Niedermeyer, E. M., Schefuß, E., Sessions, A. L., Mulitza, S., Mollenhauer, G., Schulz, M., et al. 2010. Orbital- and millennial-scale changes in the hydrologic cycle and vegetation in the western African Sahel: insights from individual plant wax δD and δ13C. *Quat. Sci. Rev.* 29(23–24):2996–3005, doi:10.1016/j.quascirev.2010.06.039

Numaguti, A. (1999). Origin and recycling processes of precipitating water over the eurasian continent: Experiments using an atmospheric general circulation model. *J. Geophys. Res.* 104, 1957. doi:10.1029/1998jd200026

Pearson, P. N., Foster, G. L., and Wade, B. S. (2009). Atmospheric carbon dioxide through the Eocene–Oligocene climate transition. *Nature* 461 (7267), 1110–1113. doi:10.1038/nature08447

Pedentchouk, N., Sumner, W., Tipple, B., and Pagani, M. (2008). δ13C and δD compositions of n-alkanes from modern angiosperms and conifers: An experimental set up in central Washington State, USA. *Org. Geochem.* 39 (8), 1066–1071. doi:10.1016/j.orggeochem.2008.02.005

Peters, K. E., and Moldowan, J. M. (1993). *The biomarker guide: Interpreting molecular fossils in Petroleum and ancient sediments[J].* Englewood Cliffs Nj: Prentice-Hall.

Ramstein, G., Fluteau, F., Besse, J., and Joussaume, S. (1997). Effect of orogeny, plate motion and land–sea distribution on Eurasian climate change over the past 30 million years. *Nature* 386 (6627), 788–795. doi:10.1038/386788a0

Raymo, M. E., Ruddiman, W. F., and Froelich, P. N. (1988). Influence of late Cenozoic mountain building on ocean geochemical Cycles. *Geol.* 16, 649–653. doi:10.1130/0091-7613(1988)016<0649:iolcmb>2.3.co;2

Raymo, M. E., and Ruddiman, W. F. (1992). Tectonic forcing of late cenozoic climate. *Nature* 359, 117–122. doi:10.1038/359117a0

Ruddiman, W. F., and Kutzbach, J. E. (1989). Forcing of late Cenozoic northern hemisphere climate by plateau uplift in southern Asia and the American west. *J. Geophys. Res.* 94 (D15), 18409–18427. doi:10.1029/jd094id15p18409

Ruddiman, W. F., and Kutzbach, J. E. (1991). plateau uplift and climatic change. *Sci. Am.* 264, 66–75. doi:10.1038/scientificamerican0391-66

Sage, R. E. (2001). *Environmental and evolutionary preconditions for the origin and diversification of C4 photosynthetic syndrome*. Blackwell Publishing Ltd.

Sato, T. (2009). Influences of subtropical jet and Tibetan Plateau on precipitation pattern in Asia: Insights from regional climate modeling. *Quat. Int.* 194, 148–158. doi:10.1016/j.quaint.2008.07.008

Sato, T., and Kimura, F. (2005). Impact of diabatic heating over the Tibetan Plateau on subsidence over northeast Asian arid region. *Geophys. Res. Lett.* 32 (5), L05809. doi:10.1029/2004gl022089

Schubert, B. A., and Jahren (2012). The effect of atmospheric CO2 concentration on carbon isotope fractionation in C3 land plants. *Geochim. Cosmochim. Acta* 96, 29–43. doi:10.1016/j.gca.2012.08.003

Sorrel, P., Eymard, I., Leloup, P.-H., Maheo, G., Olivier, N., Sterb, M., et al. (2017). Wet tropical climate in SE Tibet during the late Eocene. *Sci. Rep.* 7 (1), 7809–7811. doi:10.1038/s41598-017-07766-9

Spicer, R. A. (2017). Tibet, the Himalaya, Asian monsoons and biodiversity in what ways are they related? *Plant Divers.* 39 (5), 233–244. doi:10.1016/j.pld.2017.09.001

Steinthorsdottir, M., Vajda, V., Pole, M., and Holdgate, G. (2019). Moderate levels of Eocene pCO2 indicated by Southern Hemisphere fossil plant stomata. *Geology* 47 (10), 914–918. doi:10.1130/g46274.1

Su, T., Spicer, R. A., Li, S. H., Huang, J., Sherlock, S., Huang, Y. J., et al. (2018). Uplift, climate and biotic changes at the Eocene-Oligocene transition in south-eastern Tibet. *Natl. Sci. Rev.* 6 (3), 495–504. doi:10.1093/nsr/nwy062

Su, T., Spicer, R. A., Li, S. H., Xu, H., Huang, J., Sherlock, S., et al. (2019). Uplift, climate and biotic changes at the Eocene–Oligocene transition in south-eastern Tibet. *Natl. Sci. Rev.* 6(3), 495–504, doi:10.1093/nsr/nwy062

Sun, Jimin, and Jia (2015). *Paleoelevation of Tibetan Lunpola basin in the Oligocene-Miocene transition estimated from leaf wax lipid dual isotopes[J].* Global & Planetary Change

Sun, J., Windley, B. F., Zhang, Z., Fu, B., and Li, S. (2016). Diachronous seawater retreat from the southwestern margin of the Tarim Basin in the late Eocene. *J. Asian Earth Sci.* 116, 222–231. doi:10.1016/j.jseaes.2015.11.020

Sun, Q., Xie, M., Shi, L., Zhang, Z., Lin, Y., Shang, W., et al. (2013). Alkanes, compound-specific carbon isotope measures and climate variation during the last millennium from varved sediments of Lake Xiaolongwan, northeast China. *J. Paleolimnol.*, 50:331–344, doi:10.1007/s10933-013-9728-4

Tapponnier, P., Zhiqin, X., Roger, F., Meyer, B., Arnaud, N., Wittlinger, G., et al. (2001). Oblique stepwise rise and growth of the Tibet plateau. *Science* 294 (5547), 1671–1677. doi:10.1126/science.105978

Tipple, B. J. (2010). Carbon isotope ratio of cenozoic CO2: A comparative evaluation of available geochemical proxies[J]. *Paleoceanography* 25. doi:10.1029/2009PA001851

Vicentini, A., Barber, J. C., Aliscioni, S. S., Giussani, L., and Kellogg, E. (2008). The age of the grasses and clusters of origins of C4 photosynthesis[J]. *Glob. Change Biol.* 14 (12), 2963–2977. doi:10.1111/j.1365-2486.2008.01688.x

Walker, J. C. G., Hays, P. B., and Kasting, J. F. (1981). A negative feedback mechanism for the long-term stabilization of Earth's surface temperature. *J. Geophys. Res.* 86, 9776–9782. doi:10.1029/jc086ic10p09776

Wang, Jia, Axia, Wang, G., Zhou, L., Jia, Y., et al. (2018). Temperature effect on abundance and distribution of leaf wax n-alkanes across a temperature gradient along the 400 mm isohyet in China. *Org. Geochem.* 120, 31–41. doi:10.1016/j.orggeochem.2018.03.009

Wang, Q., Wyman, D. A., Xu, J. F., Dong, Y., Vasconcelos, P. M., Pearson, N., et al. (2008). Eocene melting of subducting continental crust and early uplifting of central Tibet: Evidence from central-western Qiangtang high-K calc-alkaline andesites, dacites and rhyolites. *Earth Planet. Sci. Lett.* 272:158-171, doi:10.1016/j.epsl.2008.04.034

Wang, Y. (2006). *The characteristics and climatic significance of biomarkers in modern soil and lacustrine sediments in the north-south climate zone of East Asia[D].* Lanzhou University.

Wang, C., Dai, J., Zhao, X., Li, Y., Graham, S. A., He, D., et al. (2014). Outward-growth of the Tibetan Plateau during the Cenozoic: A review. *Tectonophysics* 621, 1–43, doi:10.1016/j.tecto.2014.01.036

Wei, W., Lu, Y., Xing, F., Liu, Z., Pan, L., and Algeo, T. J. (2017). Sedimentary facies associations and sequence stratigraphy of source and reservoir rocks of the

lacustrine Eocene Niubao Formation (Lunpola Basin, central Tibet). *Mar. Pet. Geol.* 86, 1273–1290. doi:10.1016/j.marpetgeo.2017.07.032

Xie, S., Chen, F. H., Wang, Z. Y., Gu, Y., and Huang, Y. (2003a). Lipid distributions in loess paleosol sequences from North West China. *Org. Geochem.* 34, 1071–1079. doi:10.1016/s0146-6380(03)00083-4

Xie, S., Huang, J., and Wang, H. 2005. Paleoclimatic significance of fatty acids in stalagmites from Qingjiang and Shangdong, Hubei Province[J].*Science in China(Series D:Earth Sciences)* (03):246–251.

Xie, S., Yao, T., and Kang, S. 1999. Thompson.Climatic and environmental implications from organic matter in Dasuopu glacier in Xixiabangma in Qinghai-Tibetan Plateau[J].*Science in China(Series D:Earth Sciences)* (04):383–391.

Xie, S., Liang, B., Guo, J., Yi, Y., Evershed, R. P., Maddy, D., et al. (2003b). Biomarker compounds and related global changes [J]. *Quat. Res.* (05), 521–528.

Xu, X., Dong, L., Zhao, Y., and Wang, Y. (2019). Effect of the asian water tower over the qinghai-tibet plateauand the characteristics of atmospheric water circulation. *Chin. Sci. Bull.* 62 (27), 2830–2841. doi:10.1360/tb-2019-0203

Yang, P., Zhang, H. C., and Wang, Y. L. (2011b). . Climatic and environmental implications from n-alkanes in glacially eroded lake sediments in Tibetan Plateau: An example from Ximen Co[J]. *Chinese Science Bulletin* 056(014):P.1503-1510.

Yang, P., Zhang, H., Wang, Y., Lei, G., Nace, T., and Zhang, S. (2011a). Information on climate and environmental changes recorded by n-alkanes in glacial lake sediments on the Qinghai-Tibet plateau: A case study of jimenco[J]. *Chin. Sci. Bull.* 56 (14), 1132–1139.

Yatagai, A., and Yasunari, T. (1998). Variation of summer water vapor transport related to precipitation over and around the arid region in the interior of the Eurasian continent. *J. Meteorological Soc. Jpn.* 76, 799–815. doi:10.2151/jmsj1965.76.5_799

Ye, C., Yang, Y., Fang, X., Zhang, W., Song, C., and Yang, R. (2020). Paleolake salinity evolution in the Qaidam Basin (NE Qinghai-Tibet plateau) between ~42 and 29 Ma: Links to global cooling and Paratethys Sea incursions[J]. *Sediment. Geol.*, 409. (prepublish).

Yuan, Q., Vajda, V., Li, Q-K., Fan, Q-S., Wei, H-C., Qin, Z-J., et al. (2016). A late Eocene palynological record from the Nangqian basin, Qinghai-Tibet plateau: Implications for stratigraphy and paleoclimate[J]. *Palaeoworld* 26 (2), S1871174X16301020. doi:10.1016/j.palwor.2016.10.003

Yuan, Q., Natasha, B., Catarina, R., Gao, D. L., Wei, H. C., Fan, Q. S., et al. (2020). Aridification signatures from fossil pollen indicate a drying climate in east-central Tibet during the late Eocene. *Clim. Past.* 16 (6), 2255–2273. doi:10.5194/cp-16-2255-2020

Zachos, J. C., and Kump, L. R. (2005). Carbon Cycle feedbacks and the initiation of Antarctic glaciation in the earliest Oligocene. *Glob. Planet. Change* 47, 51–66. doi:10.1016/j.gloplacha.2005.01.001

Zachos, J., Pagani, M., Sloan, L., Thomas, E., and Billups, K. (2001). Trends, rhythms, and aberrations in global climate 65 Ma to present. *Sci. (New York, N.Y.)* 292 (5517), 686–693. doi:10.1126/science.1059412

Zhang, Z. H., Zhao, M., Eglinton, G., Lu, H., and Huang, C. (2006). Leaf wax lipids as paleovegetational and paleoenvironmental proxies for the Chinese Loess Plateau over the last 170 kyr. *Quat. Sci. Rev.* 25, 575–594. doi:10.1016/j.quascirev.2005.03.009

Zhang, Z., Wang, H., Guo, Z., and Jiang, D. (2007). What triggers the transition of palaeoenvironmental patterns in China, the Tibetan Plateau uplift or the Paratethys Sea retreat? *Palaeogeogr. Palaeoclimatol. Palaeoecol.* 245, 317–331. doi:10.1016/j.palaeo.2006.08.003

Zhang, W., Fang, X., Zhang, T., Song, C., and Yan, M. (2020). Eocene rotation of the northeastern central Tibetan plateau indicating stepwise compressions and eastward extrusions. *Geophys. Res. Lett.* 47 (17). doi:10.1029/2020gl088989

Zheng, Y., Zhou, W., Meyers, P. A., and Xie, S. (2007). Lipid biomarkers in the Zoigê-Hongyuan peat deposit: Indicators of Holocene climate changes in West China. *Org. Geochem.* 38 (11), 1927–1940. doi:10.1016/j.orggeochem.2007.06.012